

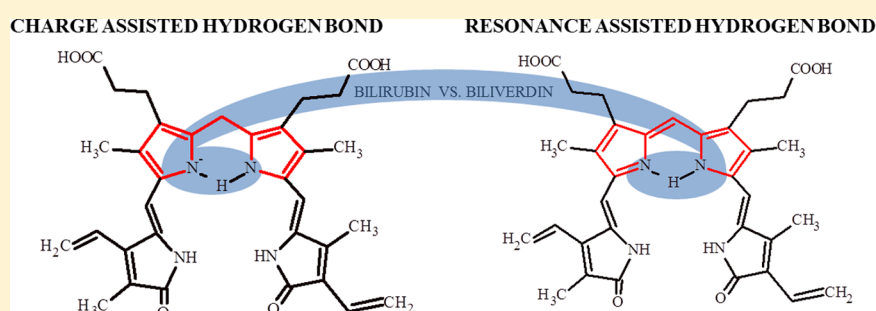
Comparison of Resonance Assisted and Charge Assisted Effects in Strengthening of Hydrogen Bonds in Dipyrrens

Jarosław J. Panek,[†] Aneta Jezierska-Mazzarello,[†] Paweł Lipkowski,[‡] Agata Martyniak,[†] and Aleksander Filarowski^{*,†}

[†]Faculty of Chemistry, University of Wrocław, F. Joliot-Curie 14, 50-383 Wrocław, Poland

[‡]Theoretical Chemistry Group, Institute of Physical and Theoretical Chemistry, Wrocław University of Technology, Wyb. Wyspiańskiego 27, 50-370 Wrocław, Poland

S Supporting Information



ABSTRACT: This paper deals with the study of two types of hydrogen bonding: a quasi-aromatic hydrogen bonding in dipyrromethane and the ionic one in dipyrromethane. The study focuses on two phenomena—the proton transfer process and tautomeric equilibrium. Metric parameters and spectroscopic assignments have been calculated; this allowed a further comparison of spectral features calculated with four methods (Car–Parrinello molecular dynamics (CPMD), ab initio, density functional theory (DFT), and numerical calculation of anharmonic vibrational levels via a solution of the corresponding 1D Schrödinger equation). A significant dynamics of the bridged proton and bent vibration of pyrrole fragments in dipyrromethane have been exposed by the CPMD calculations. The prevailing of the ionic effect over the π -electronic coupling in the strengthening of the hydrogen bonding has been shown on the basis of the calculated structural, electron-topological, and spectral data as well as potential energy surface (PES). The analysis of the aromaticity and electronic state of pyrrole and chelate moieties depending on the tautomeric equilibrium by the quantum theory of atoms in molecules (QTAIM) method was conducted. The principle divergence in the behavior of aromaticity of the chelate chains in the analyzed compounds was demonstrated.

INTRODUCTION

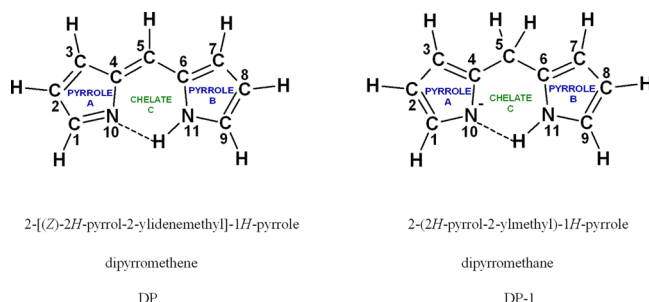
The main goal of the paper is the study of the intramolecular hydrogen bonding in dipyrrens by quantum–mechanical calculations. The biological importance of dipyrrens is remarkable as they appear as a fragment of the chlorophyll desegmentation,^{1,2} a part of porphyrin,³ and an indacene base of the BODIPY-fluorescent dye.⁴ The HEME disintegration proceeds first through bilirubin and next into biliverdin⁵ that are composed of the dipyrromethane and dipyrromethane fragments, correspondingly. The transition from bilirubin to biliverdin is grounded by stereo conformational changes and interactions like hydrogen bonds.^{6,7} Despite a great number of biological studies of polypyrroles, the description of the hydrogen bonding (HB) and proton transfer (PT) in these compounds is far from being comprehensive. This paper aims at filling this gap and presents the study of dipyrromethane (DP) and dipyrromethane (DP-1), Scheme 1, which vary basically in terms of intramolecular hydrogen bonds. The study focuses on the proton transfer process and tautomeric

equilibrium which are possible in these molecules. Dipyrromethane is the combination of two pyrroles via the methylene bridge which attenuates π -electronic conjugation between pyrrole fragments to a great extent. Dipyrromethane is the combination of two pyrroles via the methine bridge releasing a significant π -electron conjugation between pyrrolic rings. This composition introduces the so-called quasi-aromatic hydrogen bonding.⁸ The quasi-aromatic hydrogen bonding is conditioned by the intramolecular resonance effects strengthening the hydrogen bond (resonance assisted hydrogen bond, RAHB).⁹

The next object of the study is dipyrromethane which exists in anionic form, that is, with a negative charge on the molecule. Therefore, the intramolecular hydrogen bond in this compound can be referred to the so-called ionic hydrogen bond¹⁰ or the charge assisted hydrogen bonding (CAHB).¹¹ It is stated that the ionic interactions cause the strengthening of hydrogen

Received: February 6, 2013

Published: January 7, 2014

Scheme 1. Molecular Structure of the Studied Compounds^a

^aThe presence of intramolecular hydrogen bonding is indicated by the dashed line.

bonding.^{12,13} It turns, the π -electronic coupling in the NCCCCN chelate chain of dipyrromethene also strengthens the intramolecular hydrogen bond. Consequently, the main aim of this study is comparison of resonance and ionic effects on the intramolecular hydrogen bonding in the skeletons of two dipyrins with various linkages. Achieving this aim requires the use of advanced quantum chemistry methods¹⁴ (first-principles molecular dynamics,¹⁵ ab initio, DFT,^{16,17} and quantum theory of atoms in molecules (QTAIM)¹⁸). The theoretical approaches employed in the study were chosen with care for a deeper insight into the hydrogen bonding from various perspectives. The static as well as molecular dynamics models were developed to have a large database for the discussion of metric and spectroscopic interpretations of the RAHB and the CAHB present in the studied compounds. It is necessary to underline that these two kinds of hydrogen bonding were not compared before on the basis of static and time-evolution methods.

COMPUTATIONAL METHODS

Static Methods. Static models describing the metric and spectroscopic features of the studied compounds were developed on the basis of ab initio and density functional theory (DFT). This part of simulations was carried out using the Gaussian 09 suite of programs.¹⁹ First the energy minimization was performed using the Møller–Plesset second order perturbation theory (MP2)²⁰ and DFT with the B3LYP functional.^{21,22} Pople's triple- ζ valence-split basis set 6-311++G(2df,2pd) was applied during the simulations.²³ The optimized molecular structures of the studied compounds are presented in Figure 1. The pseudostable, flat structure of dipyrromethane (denoted as FDP-1) was also obtained. Harmonic frequency calculations were performed to confirm that the obtained structures correspond to the minimum on the potential energy surface (PES).

In the next step, for the investigated compounds, one-dimensional potential energy profiles were obtained as results of the calculations at selected points along the proton transfer reaction path. Four approaches were applied to study the potential energy functions of the intramolecular proton transfer: (i) the first approach is based on the stepwise elongation of the NH bond length (with 0.1–0.05 Å increment) with full optimization of the remaining metric parameters (nonadiabatic approximation); (ii and iii) the second and third approaches rests on the stepwise elongation (0.1–0.05 Å) of the HN bond length optimizing the CNH valence angle and the CCHN torsion angle, and the CNH valence angle for the fixed geometry of the investigated

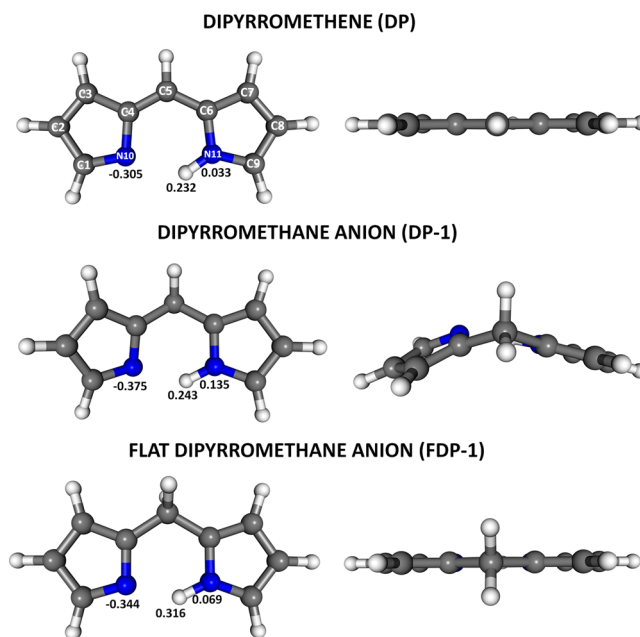


Figure 1. Molecular structures of the studied compounds obtained as a result of the geometry optimization at the MP2/6-311++G(2df,2pd) level of theory. The atoms numbering scheme is prepared according to the IUPAC convention. The values of Mulliken charges are presented for atoms involved in the intramolecular hydrogen bonding.

structures, respectively (adiabatic approximation); (iv) the fourth one is based on the stepwise elongation of the NH bond length (with 0.1–0.05 Å increment) for the fixed geometry of the studied structures (single point approximation).

Car–Parrinello Molecular Dynamics. A dynamical nature of the investigated compounds was studied using DFT-based Car–Parrinello molecular dynamics (CPMD).¹⁵ The CPMD calculations were carried out in the gas phase, with the PBE exchange–correlation functional.²⁴ Norm-conserving Troullier–Martins pseudopotentials²⁵ were applied, and the kinetic energy cutoff of the plane-wave basis set was 90 Ry. The molecules were placed in a cubic box ($a = 18$ Å). The interactions with periodic images were removed using the Hockney's scheme.²⁶ After initial structural optimization, the CPMD runs were carried out. The fictitious orbital mass of 400 au and the time step of 3 au (0.0726 fs) were used. The ionic temperature, set at 298 K, was controlled by Nosé–Hoover thermostat chains.^{27,28} The data collection, after the initial equilibration phase, lasted ca. 15 ps for both compounds. The potential of mean force, PMF, for the proton motion was calculated by direct transformation of the proton position distribution (density probability) ρ : $\text{PMF}(d) = -RT \ln \rho(d)$, where d is the chosen coordinate. Determination of vibrational features was based on the power spectra of atomic velocities.

A similar computational setup (PBE functional, plane wave basis set with 90 Ry cutoff, 3 au time step, thermostatting at 298 K) was used in a liquid phase Car–Parrinello study. A molecule of DP and anion of DP-1 were immersed in a box of 216 water molecules and the overlapping solvent molecules were removed. A cubic box of $a = 18.62$ Å (giving density of 1.0 g/cm³) with periodic boundary conditions was used in the liquid phase simulations. After initial thermalization a run of 1.8 ps was carried out for solvated DP as well as DP-1. The trajectories were then used to analyze time evolution of the

relevant structural parameters (hydrogen bridge structure, dihedral angles).

Aromaticity HOMA Index. To describe the aromaticity and quasi-aromatic formation changes upon the bridged proton movement in the studied compounds, the harmonic oscillator model of aromaticity (HOMA) index was selected as the most reliable parameter in the description of hydrogen bonding and tautomeric equilibrium:²⁹

$$\text{HOMA} = 1 - \frac{\alpha}{n} \sum_{r=1}^{n_1} (R_{\text{opt}} - R_i)^2 \quad (1)$$

where n is the number of bonds, α is an empirical constant, and R_{opt} and R_i are optimal and individual bond lengths.²⁹ Only the CO, CC, and CN bonds were taken into account for the HOMA (chelate) aromaticity index calculation. The OH and HN bonds were not taken into consideration due to the lack of the π -electronic conjugation via the hydrogen bond.

QTAIM, Mulliken, and Merz–Kollman Methods. The quantum theory atoms in molecule (QTAIM) theory¹⁸ was applied to describe the electronic structure changes and electron density in the analyzed compounds upon the structural changes introduced by the bridged proton movements. The electron density changes were studied on the basis of the electron density (ρ) at the bond critical point (BCP) and at the ring critical point (RCP). The QTAIM analysis was performed using the AIM2000 program³⁰ with all the default options. Atomic charges were calculated on the basis of the Mulliken and Merz–Kollman schemes.³¹ The Mulliken and Merz–Kollman atomic charges were calculated using the Gaussian 09¹⁹ suite of programs.

RESULTS AND DISCUSSION

Potential Energy Curve, Potential Energy Barrier vs Proton Transfer in Dipyrins. The current consensus in the literature state that calculations of potential energy surface are a reliable source of information of hydrogen bonding, spectral characteristics, and a possible reaction pathway of chemical reactions.^{32–34} The calculations of potential energy curves with respect to a few variable coordinates and conformations for the dipyrromethene and dipyrromethane are presented in this section. This part of the paper dwells on various approaches to the calculation of potential energy curves and the comparison of spectral characteristics obtained by means of different quantum–mechanical methods. To carry out this task the calculations of the structures of NH tautomeric form and transition state (TS) were performed. The calculations under the nonadiabatic approach are described—the optimization of all structural parameters except NH bond which was gradually elongated (Figure 2A).

A structural difference between dipyrromethene and dipyrromethane, visualized in Figure 1, is reflected in their electronic structure. Dipyrromethene is planar due to π -electronic conjugation in the NCCCN chelate chain which also keeps a molecule flat under the proton transfer process. As for the DP-1 compound, its structure is bent (Figure 1) and the angle between two pyrrole moieties equals 113°/115° (MP2/B3LYP). A flat structure of dipyrromethane, denoted FDP-1, was also obtained during the full geometry optimization process (Figure 1). However, the energy of this optimized pseudostable structure is higher than the energy of the bent structure of dipyrromethane on 1.80/1.07 kcal/mol (MP2/B3LYP). It is an interesting fact that the pseudostable structure of the FDP-1

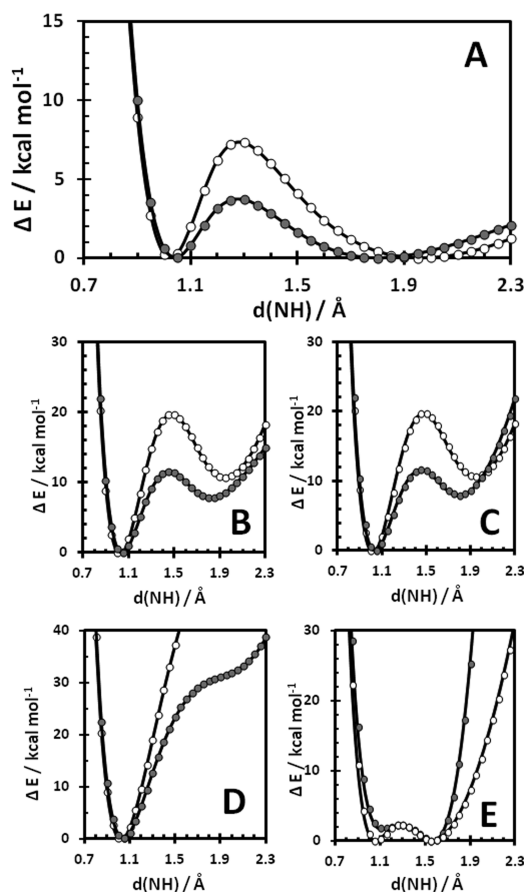


Figure 2. Calculated (MP2/6-311++G(2df,2pd)) potential energy functions of the proton displacement for dipyrromethene (DP, open circles) and dipyrromethane (DP-1, gray circles). Potential energy curves calculated at the B3LYP/6-311++G(2df,2pd) level of theory are omitted for clarity and attached as supplementary data. Potential energy functions were computed by (A) full structural optimization on stepwise elongation of the NH bond length; (B) partial structure optimization (optimized HNC and HNCC angles) on stepwise elongation of the NH bond length; (C) partial structure optimization (optimized HNC angle) on stepwise elongation of the NH bond length; (D) single point calculations of optimized structure; (E) optimized HNC angle for fixed parameters of the transition state (DP, open circles), single point calculations for fixed structural parameters of the transition state (DP, gray circles).

compound comes to be bent in the first scan ($d(\text{NH}) = 1.05 \text{ \AA}$) of the nonadiabatic approach.

The nonadiabatic approach resulted in obtaining the potential energy curves for the DP and DP-1 compounds with two energy minima with an energetic barrier equal to 7.35/9.50 and 3.69/4.76 kcal/mol (MP2/B3LYP), correspondingly (Figure 2A). The obtained potential curves point out much stronger interactions in the ionic hydrogen bond (DP-1) than those in the quasi-aromatic hydrogen bond (DP). A larger asymmetry of the nonadiabatic potential curves and a remarkably smaller energetic barrier for the proton transfer support this fact (compare nonadiabatic potential curves for the DP and DP-1 compounds). These results are also verified by the structural data which show that the hydrogen bridge length in the DP-1 compound (2.666/2.712 \AA MP2/B3LYP) is shorter than that in the DP compound (2.726/2.794 \AA MP2/B3LYP). This effect gets stronger for the nonplane configuration of dipyrromethane (Figure 2). As for the single

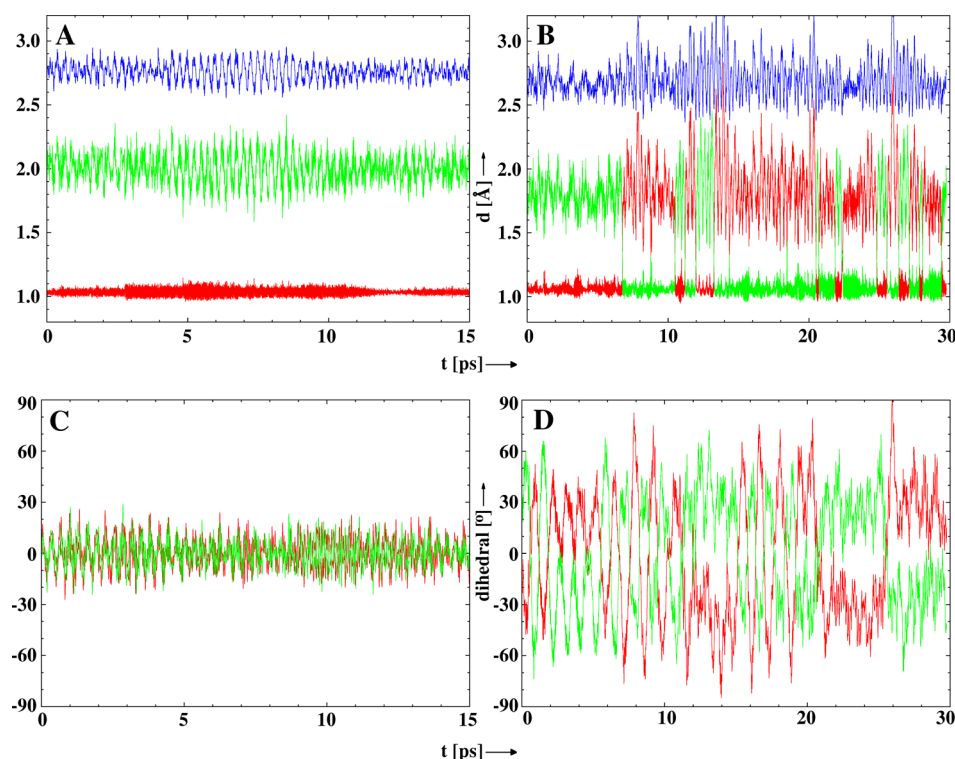


Figure 3. Time evolution of the N \cdots N, N–H, and H–N interatomic distances (Å) for the hydrogen bonds and the dihedral angles between pyrroles planes (deg) in the DP (A and C) and DP-1 (B and D) compounds—results of the CPMD simulation in the gas phase. The color coding of the graphs is as follows: (A and B) green corresponds to the $d(\text{N}\cdots\text{H})$ distance, red corresponds to the $d(\text{NH})$ distance, and blue corresponds to the $d(\text{NN})$ distance.

point approach, the potential curve is strongly different from that mentioned above due to lack of the second minimum (Figure 2D). The changes of the potential curves analyzed in the paper are in agreement with the knowledge of hydrogen bonding.³⁵

The question arises about the possibility of the intramolecular proton transfer in the studied compounds. To elucidate the situation, two phenomena have been estimated: the dynamics of the bridged proton by the CPMD method and the height of the energy barrier for the proton transfer by static DFT and ab initio methods. The performed CPMD computations have shown that the proton transfer is unlikely to occur in the DP compound. This confirmation is based on the gas-phase CPMD runs which do not reveal any event corresponding to the jump of the bridged proton to the proton-acceptor atom (Figure 3A). It is noteworthy that the height of the energy barrier calculated by the MP2 and B3LYP methods is rather significant for dipyrromethene ($\Delta E = 7.35/9.50$ kcal/mol MP2/B3LYP). The collation of the energy values for dipyrromethene and ortho-hydroxyaldimine ($\Delta E \cong 5$ kcal/mol),³⁶ where only one tautomer in nonpolar solvent was observed³⁷ makes it obvious that the proton transfer in the DP compound is scarcely probable under experimental conditions. As for dipyrromethane, the height of the energy barrier of the proton transfer in the DP-1 compound calculated by the static MP2 and B3LYP methods (3.69/4.76 kcal/mol) is less than in the DP compound (7.35/9.50 kcal/mol). According to the experimental and theoretical (B3PW91/6-31+G(d,p), PBE1PBE/6-311++G(2d,2p) and MP2/6-311++G(2d,2p)) research by Limbach³⁸ and Durlak³⁹ of the height of the energy barrier, it enables a proton transfer in the NN hydrogen

bridge of 6-nitro-2,3-dipyrrol-2-ylquinoxaline anion. Therefore the proton transfer process is possible in the DP-1 compound.

The examples of necessity of using ab initio molecular dynamics schemes, including CPMD, involve the bond breaking and forming processes and detailed studies of hydrogen bonds as it was shown in previous studies.^{40–42} The CPMD calculations showed a large mobility of the proton in the intramolecular hydrogen bridge. The gas-phase CPMD run develops a trajectory where the jump of the proton to proton-acceptor is observed several times (Figure 3B). This effect is related to the significant dynamics of the C–CH₂–C bridge. The jump of the bridged proton in the DP-1 compound is observed at the dihedral angle close to zero when the intramolecular hydrogen bond is the shortest. This situation conditions the strongest interrelations between the bridged proton and the proton-acceptor atom. In terms of the dynamics of the bent vibrations of the pyrrole fragments it is definitely weaker in the DP compound than in the DP-1 compound (cf. Figures 3C and 3D). Such a phenomenon is explained by a significant π -electronic coupling via C–CH=C bridge in the DP compound, which keeps the molecule flat.

The differences in the dynamical regimes of proton motion in the bridges of the DP and DP-1 compounds, discussed above on the basis of time evolution of the metric parameters of the hydrogen bond, are best summarized by the histograms (probability density plots based on the CPMD trajectory) presented in Figure 4. At the time when the proton, in the DP compound, is clearly localized at one of the nitrogen atoms, for the DP-1 compound, the proton is shuttled between two nitrogen atoms. This fact supports the MP2 and B3LYP calculations that the energy barrier for proton transfer is much higher in DP compound than in the DP-1 compound. It is

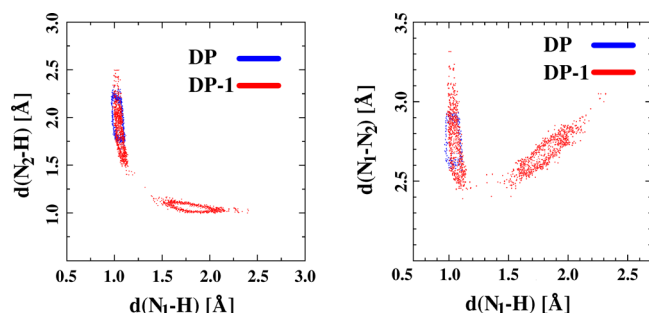


Figure 4. Separate histograms of donor-proton ($d(\text{N1-H})$) and donor-acceptor ($d(\text{N1-N2})$) distances for the DP and DP-1 compounds (DP – $\Delta d(\text{N1-H}) = 0.91\text{--}1.12$ Å and $\Delta d(\text{N1-N2}) = 2.57\text{--}2.94$ Å and DP-1 – $\Delta d(\text{N1-H}) = 0.92\text{--}2.45$ Å and $\Delta d(\text{N1-N2}) = 2.45\text{--}3.08$ Å). The isocontours are drawn at the 5 Å^{-2} probability density level.

noteworthy that the relation between the potential of mean force (PMF) for the proton motion and the density probability (ρ) provides a measure of the associated free energy profile: $\text{PMF}(d) = -RT \ln \rho(d)$, where d is the donor-proton distance, in turn, PMF corresponds to the free energy. The one-dimensional PMF profile is presented in Figure S1 in the Supporting Information, where the statistical nature of the sampling is best visible in two minima. The profile is very rugged above 2 kcal/mol because of the decreased sampling frequency of these regions in the phase space. Moreover, the energy barrier estimated by this method for the DP-1 compound is ca. 3 kcal/mol, which agrees very well with the static calculations.

The next stage of the study of the intramolecular hydrogen bond in dipyrins is an analysis of the position of the stretching band ($\nu(\text{NH})$) within the framework of CPMD, B3LYP, MP2 methods, and anharmonic treatment. The B3LYP and MP2 methods feature the following $\nu(\text{NH})$ band positions: 3462/3416 and 3172/3104 cm^{-1} for the DP and DP-1 compounds, respectively. However, the fact is stated that these calculations do not show the full coincidence with the experimental data (even taking into account only the center of gravity of a band). It is well-known that such divergence results from a marked anharmonicity of the vibration of the bridged proton.³⁵ Therefore, the shooting method applied by Stare and Mavri⁴³ to the vibrational problem and tested in a number of papers^{36,44,45} was applied for a more precise description of the $\nu(\text{NH})$ band position. Initially the potential energy curves (Figure 4) calculated by four separate approaches (Computational Methods section) were used for the calculations of energy levels and, consistently, the band positions (Table 1). The obtained position of the $\nu(\text{NH})$ band is shifted into the direction of the low frequency region regarding the values obtained by the MP2 and B3LYP methods (Table 1). To verify the calculated data the experimental results obtained by Hildebrandt et al.⁴⁶ for hexamethylpyrromethene were used.⁴⁷

The collation of the experimental and computational data shows the validity of a particular theoretical method. The data obtained with the static MP2 and B3LYP methods differ from the experimental ones on $\sim 200 \text{ cm}^{-1}$ (cf. the data from Table 1 with the literature^{46,50,51}). The anharmonic approach and the CPMD trajectory analysis provide the results which are the closest to the experimental data. It is necessary to note that the second and third approaches of PES calculations define the position of the $\nu(\text{NH})$ band which is much shifted into the low frequency region (2847 and 2849 cm^{-1} for the DP compound; 1900 and 2014 cm^{-1} for the DP-1 compound, Table 1) with respect to the experimental data.^{46,50,51} In addition, the anharmonic treatment of PES from the second and third approaches exposes the results close to the experimental data obtained in the polar solvents and in the solid state. Under such condensed-phase conditions, the anharmonicity of the $\nu(\text{NH})$ vibrations is definitely larger than in nonpolar environments, which is consistent with the obtained potential energy curves (the asymmetry is far larger for the A–D curves than for the E and F curves, Figure 5).

The comparison of the spectral data computed by the B3LYP, MP2, CPMD, and anharmonic treatment methods puts forward the following conclusion: the position of the $\nu(\text{NH})$ band of the DP-1 compound is visibly shifted into the low frequency region with respect to the position of the same band of the DP compound ($3462 \rightarrow 3172 \text{ cm}^{-1}$ (B3LYP); $3416 \rightarrow 3104 \text{ cm}^{-1}$ (MP2); $3120 \rightarrow 2850 \text{ cm}^{-1}$ (CPMD, see Figure 6); and $3065 \rightarrow 2674 \text{ cm}^{-1}$ (anharmonic treatment)). Taking into consideration that the position of the band stretching vibrations correlates with the enthalpy of the hydrogen bond formation ($\Delta H = f(\Delta\nu)^{52}$), so the energy of the intramolecular hydrogen bond in the DP-1 compound is larger than in the DP compound. The calculated bands of the stretching vibrations, serving as a measure of the hydrogen bonding energy,⁵³ reveal the following sequence: FDP-1 ($2885\text{--}3021 \text{ cm}^{-1}$) < DP-1 ($3100\text{--}3172 \text{ cm}^{-1}$) < DP ($3394\text{--}3462 \text{ cm}^{-1}$), Table 1. According to the sequence the $\nu(\text{NH})$ band position of the FDP-1 and DP-1 compounds is shifted bathochromically with respect to the DP compound. It shows that dipyrromethane is characterized by the hydrogen bond stronger than in dipyrromethene.

The simulations of hydrated DP and DP-1 (in a periodic box of water, 207 water molecules for DP, 205 for DP-1 anion) were carried out to analyze the impact of solvation on the properties of the intramolecular hydrogen bond in the studied dipyrins, as well as to investigate different models of solvent organization around the two compounds. The Figure S2 (Supporting Information) presents time evolution of the relevant structural parameters of the intramolecular hydrogen bridge (donor–proton, proton–acceptor, and donor–acceptor distances) as well as details of molecular conformation (dihedral angles responsible for the mutual orientation of the pyrrole rings). It is visible that the presence of water disturbs the intramolecular bridge, because the water molecules are

Table 1. Spectroscopic Data ($\nu_{\text{N-H}}(\text{cm}^{-1})$) Obtained by MP2/6-311++G(2df,2pd), B3LYP/6-311++G(2df,2pd), CPMD, and Shooting Methods

compound	DFT	MP2	shooting method ii approach ^a	shooting method iii approach ^a	shooting method iv approach ^a	CPMD
DP	3462	3416	2847	2849	3065	3120
DP-1	3172	3104	1900	2014	2674	2850

^aData obtained by ii–iv approach; see Computational Methodology.

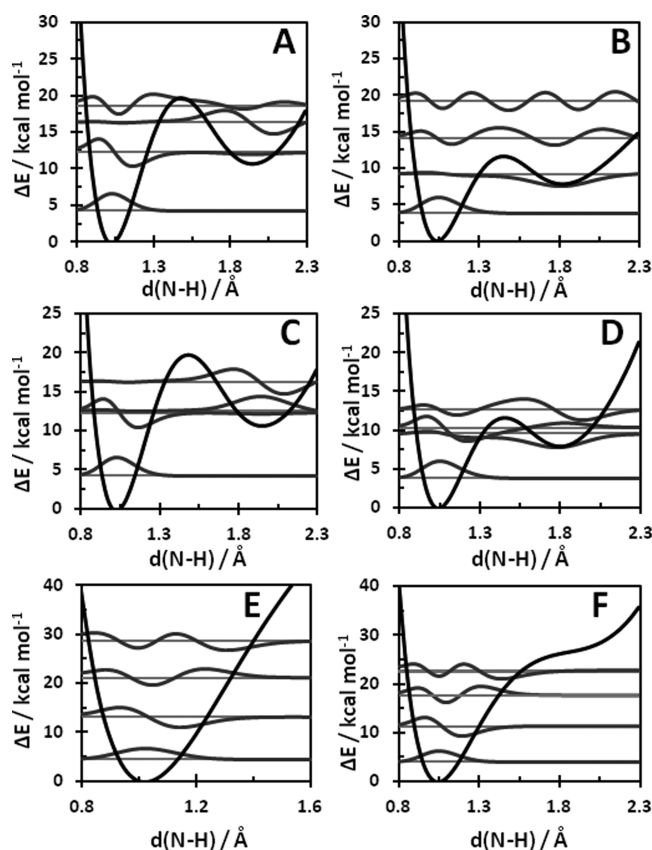


Figure 5. Potential energy curve for dipyrromethene (A, C, and E) and dipyrromethane (B, D, and F) calculated at the MP2/6-311++G(2df,2pd) level of theory and the vibrational eigenstates (0, 1, 2, and 3) together with the associated wave functions and transition energies. The A (DP) and B (DP-1) curves were obtained by the $d(\text{N-H})$ scan with optimization of the HNC and torsional HNCC angles; the C (DP) and D (DP-1) curves were prepared using the scan with optimization of the HNC angle; the E (DP) and F (DP-1) curves are obtained by single point approximation.

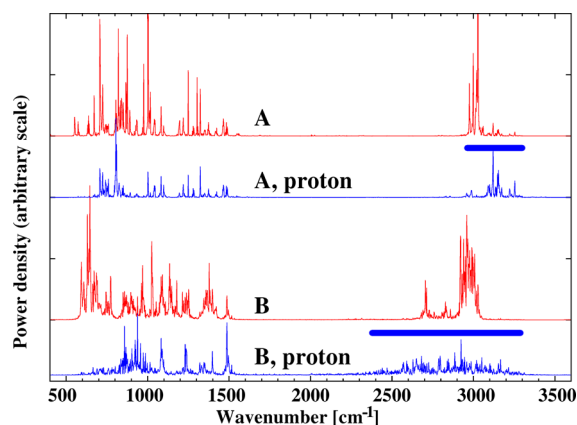


Figure 6. Atomic velocity power spectra for all atoms (red) and the hydrogen involved in the intramolecular hydrogen bond (blue) in the studied compounds (A—DP, B—DP-1) on the basis of CPMD calculations. The gravity centers of the bridged proton vibrational modes are the following: 3120 and 2850 cm^{-1} for the DP and DP-1 compounds, respectively.

competing for the bridge proton and lone pair of the acceptor nitrogen. This action is macroscopically described by very high dielectric constant of water. The action of water leads to

weakening of the intramolecular interaction, which is stronger in case of DP-1. In the gas phase, CPMD simulation of the DP-1 could exhibit a proton transfer between the two nitrogen atoms; this behavior is not observed in the liquid. Moreover, the donor–acceptor contact is lost between the 1.0 and 1.3 ps of the simulation time. This can be understood in terms of the macroscopic electric shielding. The charge-assisted bond of DP-1 is weakened much more than the resonance-assisted bridge of DP, because the charge assistance involves partially a “through-space mechanism” (electrostatics) disturbed by the presence of water. While the hydrogen bridge of DP is also surrounded by the water molecules, its strengthening is induced by the “through-bond mechanism” (resonance), which is *not* disturbed. This fact is also visible in the changes of the dihedral angles: the DP frame remains much more rigid, while the DP-1 undergoes larger conformational fluctuations than in the gas phase. The weakening of the bridge is so strong that the bridge can be broken (“unlocked”) and the conformational changes of DP-1 are increased. The Figure S3 (Supporting Information) corresponds to the picture of solvation from the point of view of the nitrogen atoms. The first maxima of the radial pair distribution function are at 2.8–2.9 Å for DP and 2.55–2.75 Å for DP-1. These correspond to a single water molecule (see the integrated radial distribution, which reaches 1 at a value of more than 3 Å) which is interacting with the hydrogen bridge. The split maximum is the result of unequal role of the two nitrogen atoms, one of which can be a proton donor, while the other—an acceptor. It is however important to note that the closest maxima for DP-1 are located at significantly smaller distances than for DP. This means that the charged DP-1 is organizing the solvent around itself stronger than DP, according to our expectations. This also explains why the impact of the water molecules on the bridge of DP-1 is stronger than for DP.

According to presented CPMD calculations, the presence of solvent weakens the hydrogen bridges in both DP and DP-1 anion, but the weakening is much stronger in the DP-1 anion. We attribute this to the fact that the charge-assisted interaction in DP-1 anion, propagating “through space”, is screened much stronger by water than the resonance-assisted interaction in DP, which propagates through chelate chain.

Comparison of Energy of Ionic and Quasi-aromatic Hydrogen Bonds. At the beginning of the discussion it should be noted that the estimation of the absolute energy of the intramolecular hydrogen bond is difficult to perform experimentally.⁵⁴ Therefore, the aim of this section is the relative comparison of the energy of hydrogen bonding in the studied compounds. The calculations of the hydrogen bond energy were carried out with the formulas described in refs 55 (eqs 2–4) and 56 (eqs 5–11)

$$E_{\text{HB}} = 6.4 \times 10^3 e^{-3.1d(\text{H}\cdots\text{N})} \quad (\text{\AA}) \quad (2)$$

$$E_{\text{HB}} = 3.8 \times 10^3 e^{-2.73d(\text{H}\cdots\text{N})} \quad (\text{\AA}) \quad (3)$$

$$E_{\text{HB}} = -5.554 \times 10^5 e^{-4.12d(\text{N}\cdots\text{N})} \quad (\text{\AA}) \quad (4)$$

$$E_{\text{HB}} = 186\rho_b - 2.3 \quad (e\text{\AA}^3) \quad (5)$$

$$E_{\text{HB}} = 163\rho_b \quad (e\text{\AA}^3) \quad (6)$$

$$(E_{\text{HB}} = 0.448G_b - 3.1) \quad (\text{kcal mol}^{-1} a_0^{-3}) \quad (7)$$

$$E_{\text{HB}} = 0.429G_{\text{b}} \quad (\text{kcal mol}^{-1} \text{a}_0^{-3}) \quad (8)$$

$$E_{\text{HB}} = -0.37V_{\text{b}} + 3.1 \quad (\text{kcal mol}^{-1} \text{a}_0^{-3}) \quad (9)$$

$$E_{\text{HB}} = -0.31V_{\text{b}} \quad (\text{kcal mol}^{-1} \text{a}_0^{-3}) \quad (10)$$

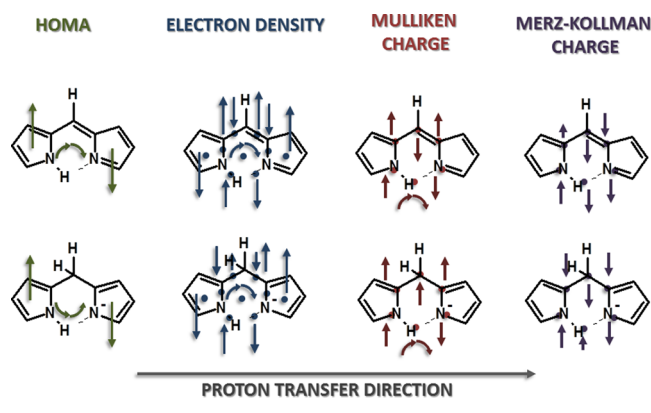
$$E_{\text{HB}} = 0.5V_{\text{b}} \quad (\text{kcal mol}^{-1} \text{a}_0^{-3}) \quad (11)$$

The examination of the values obtained with a certain method and base provides the following conclusion: the energy of the hydrogen bridge in dipyrromethane (FDP-1 and DP-1) is larger than the energy of the hydrogen bond of the dipyrromethene (DP, $\Delta E \sim 2\text{--}4$ kcal/mol, Supporting Information Table S1). The collation of the flat (FDP-1) and bent (DP-1) structures of the dipyrromethane shows that the hydrogen bridge in the FDP-1 compound is shorter than in the DP-1 compound. This phenomenon is conditioned by the interaction of the bridged proton with the lone electron pair of the proton-acceptor ($\text{H}\cdots\text{N}$), which is directed to the bridged proton (Figure 1); this leads to a much stronger attraction and a consequent shortening of the hydrogen bridge. In the DP-1 compound a dihedral angle between the plane of the pyrrole fragment of the proton-acceptor and the NH group equals 30° , which weakens the interactions in the hydrogen bridge. A similar behavior was also observed for the *ortho*-hydroxyaryl Mannich bases.⁵⁷

Aromatic and Electron-Topological Features vs Proton Transfer in Dipyrins. This section of the study deals with the estimation of the aromaticity of pyrrole and chelate fragments of the studied compounds. To complete this task, the Krygowski's HOMA aromaticity index⁵⁸ was applied, which was calculated for each point of the nonadiabatic energy curve under the stepwise proton transfer. These calculations show the decrease of the pyrrole ring aromaticity with the gradual elongation of the NH bond (Figure 7). Such tendency is observed for the both compounds (Figure 7A and B). However, the alterations for the pyrrole ring of the DP compound are more significant than for the ring of the DP-1 compound. This phenomenon is caused by the π -electronic coupling in the methene bridge of the dipyrromethene compound which leads to delocalization in the formal

single–double pair of the C4C5 and C5C6 bonds. But this effect is much weaker in the DP-1 compound due to the inhibition of the π -electronic coupling between the pyrrole rings by the methane bridge ($-\text{CH}_2-$). Thus, the dependence $\text{HOMA}(\text{pyrrole}) = f(d(\text{NH}))$ (Figure 7A and B) reveals a significant coupling between the pyrrole rings in the dipyrromethene, and it is scarcely present in the dipyrromethane. In terms of the criteria of the aromatic balance,⁵⁹ the following picture is observed for the pyrrole rings: under the proton transfer the aromaticity of one of them is growing, meanwhile the aromaticity of another one is decreasing (Scheme 2). It is interesting that the principal difference in

Scheme 2. Scheme of Changes of Aromaticity ($\text{HOMA}(\text{pyrrole})$ and $\text{HOMA}(\text{chelate})$), Electron Density (ρ_{RCP} and ρ_{BCP}), Mulliken and Merz–Kollman Atomic Charge vs Proton Transfer in Dipyrromethene and Dipyrromethane



the behavior of the chelate ring aromaticity ($\text{HOMA}(\text{chelate})$) of the studied compounds is found. The aromaticity of the chelate ring in the dipyrromethene increases as far as the transition state is concerned and then goes down under the proton transfer (Figure 7C). Such behavior of the chelate chain aromaticity is typical for the hydroxyaryl and alkyl Schiff bases with the π -electronic coupling.^{60–62} This trend exposes the growth of the delocalization of the π -component in the chelate chain under the shortening of the hydrogen bond. However, a reverse trend is observed for the dipyrromethane. The negative value of the $\text{HOMA}(\text{chelate})$ index of the chelate chain (pointing out a partial antiaromaticity)⁶³ keeps going down as far as the transition state and then starts increasing under the proton transfer (Figure 7D).

The analysis of the electron density at the critical points of the bonds (BCPs) and rings (RCPs) was performed by the Bader's method¹⁸ (quantum theory of atoms in molecules, QTAIM). Under the proton moving from the donor to acceptor atoms (the lengthening of the NH distance), the value of the electron density at critical points of the donor-containing ring ($\rho_{\text{RCP}}(\text{pyrrole})$, A ring) is decreasing, whereas $\rho_{\text{RCP}}(\text{pyrrole})$ of the adjacent pyrrole (B) moiety is increasing (Supporting Information Figure S4).

The changes of the electron density at the chelate chain under the proton transfer ($\rho_{\text{RCP}}(\text{chelate}) = f(d(\text{NH}))$, Supporting Information Figure S4B) are similar for both compounds and take a bell-shaped form. However, the difference is observed in the behavior of the $\rho_{\text{RCP}}(\text{chelate})$ parameter between the dipyrromethene and the dipyrromethane. The $\rho_{\text{RCP}}(\text{chelate})$ parameter is smaller for the DP

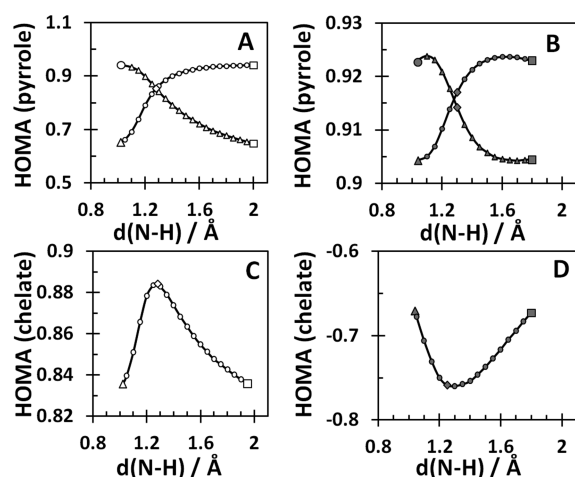


Figure 7. Correlations of the aromaticity index $\text{HOMA}(\text{pyrrole})$ and $\text{HOMA}(\text{chelate}) = f(d(\text{N-H}))$ for dipyrromethene (A and C) and dipyrromethane anion (B and D): (Δ) global minimum; (\square) transition state.

compound than for the DP-1 compound for the global energetic minimum, whereas at the transition state, the situation is reversed ($\rho_{\text{RCP}}(\text{chelate}) \text{ DP} > \rho_{\text{RCP}}(\text{chelate}) \text{ DP-1}$, Supporting Information Figure S4B). It is important to note that similar trends are also characteristic for structural parameters of the hydrogen bridge. The length of the hydrogen bridge in the DP-1 compound is shorter than the length of the hydrogen bridge in the DP compound in global energetic minimum (2.666/2.712 Å for DP-1 < 2.726/2.794 Å for DP (MP2/B3LYP)). Nevertheless, the length of the hydrogen bridges in these compounds are almost equal at the transition state (2.450/2.459 Å for DP-1 \cong 2.448/2.460 Å for DP (MP2/B3LYP)). This phenomenon is grounded by the increase of the π -electronic conjugation (the growing HOMA(chelate) index, Figure 7C) in the chelate chain of the dipyrromethene. This increase is especially intensive at the transition state which causes a marked resonance strengthening ($\text{HOMA}(\text{chelate}) = f(\Delta E)$). One should take into account that the charges on the bridged proton and nitrogen atoms (calculated by Mulliken method) undergo changes like in the $\rho_{\text{RCP}}(\text{pyrrole}) = f(d(\text{NH}))$ and $\rho_{\text{RCP}}(\text{chelate}) = f(d(\text{NH}))$ dependencies (Scheme 2). The changes described are proved by experimental results commonly accepted for the systems with hydrogen bonds.^{64,65}

CONCLUSION

A general summary of this study is that the charge assisted hydrogen bond is stronger than the resonance assisted hydrogen bond at the global energy minimum for the studied compounds. Therefore, this strengthening of hydrogen bond by means of the charge assisted (ionic) effect prevails over the strengthening by resonance assisted (π -electronic conjugation) effect at the global minimum. However, it is important that the increasing π -electronic coupling (the increase of the HOMA(chelate) index) brings about the strengthening of hydrogen bond (the $d(\text{NN})$ distance) in the DP compound. Under the proton transfer process, the strongest shortening of hydrogen bond is observed for the DP compound at the transition state. The hydrogen bond lengths are much the same for the DP and DP-1 compounds at the transition state, meanwhile at the global minimum $d(\text{DP}) > d(\text{DP-1})$. These data suggest that the strengthening of the hydrogen bond by π -electronic coupling in the chelate chain is the most efficient at the transition state.

A larger impact of the CAHB over RAHB is also present in the spectroscopic interpretations, where positions of the NH bands are more red-shifted in the DP-1 compound than in the DP compound (ab initio, DFT, anharmonic treatment, and CPMD results), and the band is much broader (CPMD result).

In conclusion, we would like to underline that the calculations by the MP2/6-311++G(2df,2pd), B3LYP/6-311++G(2df,2pd), CPMD, and QTAIM methods performed in this study lead to the agreeing results.

ASSOCIATED CONTENT

Supporting Information

Additional data related to the CPMD simulations in the gas phase (potential of mean force), full description of the liquid phase CPMD simulation, and tabulated energies of the hydrogen bond energies calculated from eqs 2–11. This material is available free of charge via the Internet at <http://pubs.acs.org>.

AUTHOR INFORMATION

Corresponding Author

*E-mail: aleksander.filarowski@chem.uni.wroc.pl. Phone number: (+48) 71-3757-229. Fax: (+48) 71-3282-348.

Notes

The authors declare no competing financial interest.

ACKNOWLEDGMENTS

This article is dedicated to Professor Benjamin J. van der Veken on the occasion of his 65th birthday. The Authors acknowledge the Wrocław Center for Networking and Supercomputing (WCSS) for generous grants of computer time. A.J.-M. and J.J.P. gratefully acknowledge the Academic Computer Center (TASK) in Gdańsk for providing computer time and facilities.

REFERENCES

- (1) Wood, T. A.; Thompson, A. Advances in the Chemistry of Dipyrins and Their Complexes. *Chem. Rev.* **2007**, *107*, 1831–1861.
- (2) Dammeyer, T.; Frankenberg-Dinkel, N. Function and distribution of bilin biosynthesis enzymes in photosynthetic organisms. *Photochem. Photobiol. Sci.* **2008**, *7*, 1121–1130.
- (3) Lindsey, J. S. Synthetic Routes to meso-Patterned Porphyrins. *Acc. Chem. Res.* **2010**, *43*, 300–311.
- (4) Boens, N.; Leen, V.; Dehaen, W. Fluorescent indicators based on BODIPY. *Chem. Soc. Rev.* **2012**, *41*, 1130–1172.
- (5) Hou, S.; Reynolds, M. F.; Horrigan, F. T.; Heinemann, S. H.; Hoshi, T. Reversible Binding of Heme to Proteins in Cellular Signal Transduction. *Acc. Chem. Res.* **2006**, *39*, 918–924.
- (6) Chen, C.; Lighner, D. A. Hemirubin: An Intramolecularly Hydrogen-Bonded Analogue for One-half Bilirubin. *J. Org. Chem.* **1998**, *63*, 2665–2675.
- (7) Chepelev, L. L.; Beshara, C. S.; MacLean, P. D.; Hatfield, G. L.; Rand, A. A.; Thompson, A.; Wright, J. S.; Barclay, L. R. C. Polypyrrroles as Antioxidants: Kinetic Studies on Reactions of Bilirubin and Biliverdin Dimethyl Esters and Synthetic Model Compounds with Peroxyl Radicals in Solution. Chemical Calculations on Selected Typical Structures. *J. Org. Chem.* **2006**, *71*, 22–30.
- (8) Lutskii, A. E.; Marchenko, T. N. In *Vodorodnaya svyaz' (Hydrogen bond)*; Sokolov, N. D., Ed.; Nauka: Moscow, 1981, p 50.
- (9) Gilli, G.; Gilli, P. The Nature of the Hydrogen Bond. *Outline of a Comprehensive Hydrogen Bond Theory*; Oxford University Press: Oxford, 2009.
- (10) Meot-Ner (Mautner), M. The Ionic Hydrogen Bond. *Chem. Rev.* **2005**, *105*, 213–284.
- (11) Gilli, G.; Gilli, P. Towards a unified hydrogen-bond theory. *J. Mol. Struct.* **2000**, *552*, 1–15.
- (12) D'Oria, E.; Novoa, J. J. Cation–Anion Hydrogen Bonds: A New Class of Hydrogen Bonds That Extends Their Strength beyond the Covalent Limit. A Theoretical Characterization. *J. Phys. Chem. A* **2011**, *115*, 13114–13123.
- (13) D'Oria, E.; Novoa, J. J. The strength–length relationship at the light of ab initio computations: does it really hold? *Cryst. Eng. Commun.* **2004**, *6*, 368–376.
- (14) *Encyclopedia of Computational Chemistry*; Schleyer, P. v R., Allinger, N. L., Clark, T., Gasteiger, J., Kollman, P. A., Schaefer, H. F., III, Schreiner, P. R., Eds.; J. Wiley and Sons: Chichester, U.K., 1998.
- (15) Car, R.; Parrinello, M. M. Unified Approach for Molecular Dynamics and Density-Functional Theory. *Phys. Rev. Lett.* **1985**, *22*, 2471–2474.
- (16) Hohenberg, P.; Kohn, W. Inhomogeneous Electron Gas. *Phys. Rev. B* **1964**, *136*, 864–871.
- (17) Kohn, W.; Sham, L. Self-Consistent Equations Including Exchange and Correlation Effects. *Phys. Rev. A* **1965**, *140*, 1133–1138.
- (18) Bader, R. F. W. *Atoms in Molecules: A Quantum Theory*; Oxford University Press: New York, 1990.
- (19) Frisch, M. J. et al. *Gaussian 09*, Revision B01; Gaussian, Inc.: Wallingford CT, 2009.

- (20) Møller, C.; Plesset, M. S. Note on an Approximation Treatment for Many-Electron Systems. *Phys. Rev.* **1934**, *46*, 618–622.
- (21) Becke, A. D. Density-functional thermochemistry. III. The role of exact exchange. *J. Chem. Phys.* **1993**, *98*, 5648–5652.
- (22) Lee, C.; Yang, W.; Parr, R. G. Development of the Colle-Salvetti correlation-energy formula into a functional of the electron density. *Phys. Rev. B* **1988**, *15*, 785–789.
- (23) Krishnan, R.; Binkley, J. S.; Seeger, R.; Pople, J. A. Self-consistent molecular orbital methods. XX. A basis set for correlated wave functions. *J. Chem. Phys.* **1980**, *72*, 650–654.
- (24) Perdew, J. P.; Burke, K.; Ernzerhof, M. Generalized Gradient Approximation Made Simple. *Phys. Rev. Lett.* **1996**, *77*, 3865–3868.
- (25) Troullier, N.; Martins, J. L. Efficient pseudopotentials for plane-wave calculations. *Phys. Rev. B* **1991**, *43*, 1993–2006.
- (26) Hockney, R. W. The potential calculation and some applications. *Meth. Comput. Phys.* **1970**, *9*, 136–211.
- (27) Nosé, S. A unified formulation of the constant temperature molecular dynamics methods. *J. Chem. Phys.* **1984**, *81*, 511–519.
- (28) Hoover, W. G. Canonical dynamics: Equilibrium phase-space distributions. *Phys. Rev. A* **1985**, *31*, 1695–1697.
- (29) Krygowski, T. M.; Cyrański, M. K. Structural Aspects of Aromaticity. *Chem. Rev.* **2001**, *101*, 1385–1419.
- (30) Biegler-König, J.; Schönbohm, D.; Bayles, D. AIM2000. *J. Comput. Chem.* **2001**, *22*, 545–559.
- (31) Mulliken, R. S. Electronic Population Analysis on LCAOMO Molecular Wave Functions. *J. Chem. Phys.* **1955**, *23*, 1833–1831.
- (32) Besler, B. H.; Merz, K. M., Jr.; Kollman, P. A. *J. Comput. Chem.* **1990**, *11*, 431.
- (33) Singh, U. C.; Kollman, P. A. *J. Comput. Chem.* **1984**, *5*, 129.
- (32) Basilevsky, M. V.; Vener, M. V. Theoretical investigations of proton and hydrogen atom transfer in the condensed phase. *Usp. Khim.* **2003**, *72*, 3–39.
- (33) Markle, T. F.; Tenderholt, A. F.; Mayer, J. M. Probing Quantum and Dynamic Effects in Concerted Proton–Electron Transfer Reactions of Phenol–Base Compounds. *J. Phys. Chem. B* **2012**, *116*, 571–584.
- (34) Majerz, I.; Olovsson, I. Proton transfer in the intramolecular NHN⁺ bonds in proton sponges with different hydrogen bridge flexibility. *Phys. Chem. Chem. Phys.* **2009**, *11*, 1297–1302.
- (35) Sandorfy, C. Recent Developments in Theory and Experiments. In *The Hydrogen Bond*; Schuster, P., Zundel, G., Sandorfy, C., Eds.; North-Holland: Amsterdam, 1976; Vol. 2.
- (36) Filarowski, A.; Koll, A.; Hansen, P.-E.; Kluba, M. Density Functional Theory Study of Intramolecular Hydrogen Bonding and Proton Transfer in o-Hydroxyaryl Ketimines. *J. Phys. Chem. A* **2008**, *112*, 3478–3485.
- (37) Rospenk, M.; Król-Starzomska, I.; Filarowski, A.; Koll, A. Proton transfer and self-association of sterically modified Schiff bases. *Chem. Phys.* **2003**, *287*, 113–124.
- (38) Pietrzak, M.; Try, A. C.; Andrioletti, B.; Sessle, J. L.; Anzenbacher, P., Jr.; Limbach, H. -H. The Largest 15N–15N Coupling Constant Across an NHN Hydrogen Bond. *Angew. Chem., Int. Ed. Engl.* **2008**, *47*, 1123–1126.
- (39) Durlak, P.; Latajka, Z. Car–Parrinello and path integral molecular dynamics study of the intramolecular hydrogen bond in the novel class of anionic H-chelates: 6-Nitro-2,3-dipyrrol-2-ylquinoxaline anion. *Chem. Phys. Lett.* **2009**, *480*, 173–177.
- (40) Jezierska, A.; Panek, J. J. First-Principle Molecular Dynamics Study of Selected Schiff and Mannich Bases: Application of Two-Dimensional Potential of Mean Force to Systems with Strong Intramolecular Hydrogen Bonds. *J. Chem. Theory Comput.* **2008**, *4*, 375–384.
- (41) Dopieralski, P. P.; Perrin, C. L.; Latajka, Z. On the Intramolecular Hydrogen Bond in Solution: Car–Parrinello and Path Integral Molecular Dynamics Perspective. *J. Chem. Theory Comput.* **2011**, *7*, 3505–3513.
- (42) Jezierska, A.; Panek, J. J.; Filarowski, A. Molecular Properties Investigation of a Substituted Aromatic Mannich Base: Dynamic and Static Models. *J. Chem. Inf. Model* **2007**, *47*, 818–831.
- (43) Stare, J.; Mavri, J. Numerical solving of the vibrational time-independent Schrödinger equation in one and two dimensions using the variational method. *Comput. Phys. Commun.* **2002**, *143*, 222–240.
- (44) Brela, M.; Stare, J.; Pirc, G.; Sollner-Dolenc, M.; Boczar, M.; Wójcik, M. J.; Mavri, J. Car–Parrinello Simulation of the Vibrational Spectrum of a Medium Strong Hydrogen Bond by Two-Dimensional Quantization of the Nuclear Motion: Application to 2-Hydroxy-5-nitrobenzamide. *J. Phys. Chem. B* **2012**, *116*, 4510–4518.
- (45) Stare, J.; Panek, J.; Eckert, J.; Grdadolnik, J.; Mavri, J.; Hadži, D. Proton Dynamics in the Strong Chelate Hydrogen Bond of Crystalline Picolinic Acid N-Oxide. A New Computational Approach and Infrared, Raman and INS Study. *J. Phys. Chem.* **2008**, *112*, 1576–1586.
- (46) Mroginski, M. -A.; Németh, K.; Bauschlicher, T.; Klotzbücher, W.; Goddard, R.; Heinemann, O.; Hildebrandt, P.; Mark, F. Calculation of Vibrational Spectra of Linear Tetrapyrroles. 3. Hydrogen-Bonded Hexamethylpyrromethene Dimers. *J. Phys. Chem.* **2005**, *109*, 2139–2150.
- (47) The studied compounds are rather unstable. The DP compound is very reactive;⁴⁸ whereas the DP-1 compound is subjected to diprotonation, which provokes either the disruption of the intramolecular hydrogen bond or the formation of the anion stabilized by two intermolecular hydrogen bonds.⁴⁹
- (48) Rohand, T.; Dolusic, E.; Ngo, T. H.; Maes, W.; Dehaen, W. Efficient synthesis of aryldipyrromethanes in water and their application in the synthesis of corroles and dipyrromethenes. *ARKIVOK* **2007**, *10*, 307–324.
- (49) Shin, J. -Y.; Patrick, B. O.; Dolphin, D. Conformational flexibility of dipyrromethenes: supramolecular assemblies with hydroquinones. *Cryst. Eng. Commun.* **2008**, *10*, 960–962.
- (50) Badger, G. M.; Harris, R. L. N.; Jones, R. A.; Sasse, J. M. Porphyrins. Part I. Intramolecular hydrogen bonding in pyrromethenes and porphyrins. *J. Chem. Soc.* **1962**, *58*, 4329–4337.
- (51) Guy, R. W.; Jones, R. A. Pyrrole studies. VIII. The NH stretching frequencies of substituted pyrroles Acetyl and benzoyl substituents. *Aust. J. Chem.* **1966**, *19*, 107–113.
- (52) Hadži, D.; Bratos, S. Vibrational spectroscopy of the hydrogen bond. In *The Hydrogen Bond. Recent Developments in Theory and Experiments*; Schuster, P., Zundel, G., Sandorfy, C., Eds.; North-Holland: Amsterdam, Netherlands, 1976; Vol. 2.
- (53) Schuster, P. In *The Hydrogen Bond*; Schuster, P., Zundel, G., Sandorfy, C., Eds.; North-Holland: Amsterdam, 1976; Vol. 2.
- (54) Korth, H. -G.; de Heer, M. I.; Mulder, P. A. DFT Study on Intramolecular Hydrogen Bonding in 2-Substituted Phenols: Conformations, Enthalpies, and Correlation with Solute Parameters. *J. Phys. Chem. A* **2002**, *106*, 8779–8789.
- (55) Musin, R. N.; Mariam, Y. H. An integrated approach to the study of intramolecular hydrogen bonds in malonaldehyde enol derivatives and naphthazarin: trend in energetic versus geometrical consequences. *J. Phys. Org. Chem.* **2006**, *19*, 425–444.
- (56) Mata, I.; Alkorta, I.; Espinosa, E.; Molins, E. Relationships between interaction energy, intermolecular distance and electron density properties in hydrogen bonded complexes under external electric fields. *Chem. Phys. Lett.* **2011**, *507*, 185–189.
- (57) Filarowski, A.; Koll, A.; Sobczyk, L. Intramolecular Hydrogen Bonding in o-hydroxy Aryl Schiff Bases. *Curr. Org. Chem.* **2009**, *13*, 172–193.
- (58) Krygowski, T. M.; Stępień, B. T. Sigma- and Pi-Electron Delocalization: Focus on Substituent Effects. *Chem. Rev.* **2005**, *105*, 3482–3512.
- (59) Filarowski, A.; Kochel, A.; Cieślík, K.; Koll, A. Steric and aromatic impact on intramolecular hydrogen bonds in o-hydroxyaryl ketones and ketimines. *J. Phys. Org. Chem.* **2005**, *18*, 986–993.
- (60) Martyniak, A.; Majerz, I.; Filarowski, A. Peculiarities of quasi-aromatic hydrogen bonding. *RSC Adv.* **2012**, *2*, 8135–8144.
- (61) Zubatyuk, R. I.; Shishkin, O. V.; Gorb, L.; Leszczynski, J. Homonuclear versus Heteronuclear Resonance-Assisted Hydrogen Bonds: Tautomerism, Aromaticity, and Intramolecular Hydrogen Bonding in Heterocyclic Systems with Different Exocyclic Proton Donor/Acceptor. *J. Phys. Chem. A* **2009**, *113*, 2943–2952.

- (62) Houjou, H.; Shingai, H.; Yagi, K.; Yoshikawa, I.; Araki, K. Mutual Interference between Intramolecular Proton Transfer Sites through the Adjoining π -Conjugated System in Schiff Bases of Double-Headed, Fused Salicylaldehydes. *J. Org. Chem.* **2013**, *78*, 9021–9031.
- (63) Alonso, M.; Herredon, B. A universal scale of aromaticity for π -organic compounds. *J. Comput. Chem.* **2010**, *31*, 917–928.
- (64) Limbach, H. -H.; Tolstoy, P. M.; Perez-Hernandez, N.; Guo, J.; Shenderovich, I. G.; Denisov, G. S. Dendritic Amplification of Stereoselectivity of a Prolinamide-Catalyzed Direct Aldol Reaction. *Israel J. Chem.* **2009**, *49*, 199–216.
- (65) Filarowski, A.; Majerz, I. AIM Analysis of Intramolecular Hydrogen Bonding in o-Hydroxy Aryl Schiff Bases. *J. Phys. Chem.* **2008**, *112*, 3119–3126.